Turkish Journal of Electrical Engineering & Computer Sciences

http://journals.tubitak.gov.tr/elektrik/

Research Article

Turk J Elec Eng & Comp Sci
(2016) 24: 849 – 862

doi:10.3906/elk-1305-110

Walsh series modeling and estimation in sensorless position control of electrical drives

Hamidreza SHIRAZI, Jalal NAZARZADEH*
Department of Electrical Engineering, Faculty of Engineering, Shahed University, Tehran, Iran

Received: 17.05.2013 • **Accepted/Published Online:** 02.12.2013 • **Final Version:** 23.03.2016

Abstract: High-performance electrical drives can be achieved by using field-oriented controllers, which make torque and flux naturally decoupled. A conventional vector-controlled drive has the disadvantage of either requiring flux and speed sensors or being affected by rotor resistance, which varies along with the motor performance. The presented paper focuses on developing a high-performance sensorless rotor flux-oriented controller of an induction machine independent of the rotor resistance variation. This method applies spectral theory of Walsh functions, which are one of the most helpful members of piecewise constant basis functions in solving dynamic models. Inherent characteristics of Walsh functions and application of an operational matrix will make the system handy and robust against inverter switching effects.

Key words: Induction machine, vector control, parameter estimation, position control, sensorless control, spectral analysis, Walsh series

1. Introduction

Decoupling control of electromagnetic torque and flux is a desirable achievement in advanced control drives of induction machines. The amplitude and the position of the rotor flux phasor are two important variables that have to be simultaneously observed in rotor flux-oriented control (RFOC) [1]. Since the rotor flux vector varies, a high-performance electrical drive should consist of an online rotor flux observer and rotor speed estimators. As air gap flux in induction machines includes several phasor space harmonics, shaft-mounted sensors in direct control of RFOC drives have lower reliability along with extra expenses. Hence, sensorless vector control has been getting more attention among researchers as a mature technology.

Several field-oriented induction motor drive methods without rotational transducers have been proposed [2]. In [3], the authors proposed a fuzzy controller, which was applied in direct torque neuro-fuzzy control of an induction motor, taking advantage of a time-variant PI controller. The disadvantage of these methods is that the rotor resistance variation causes an error in rotor flux observation and they need the motor speed sensor [4].

Different approaches to rotor resistance estimation have been analyzed in some papers. Some methods analyze estimation of rotor resistance based on model reference adaptive systems. In these methods, an error signal detects variation effects of the time constant in a rotor circuit, which can be realized by using a rotor flux computer [4] or torque signal [5]. This method is very sensitive to motor parameters' variation, which results in low performance [6]. On the other hand, the process of estimation can be done by sampling input and output signals. Using sliding mode control [7] and Kalman filters [8] in the estimation process are some examples to be

*Correspondence: nazarzadeh@shahed.ac.ir

named. Because of noisy signals in the systems, these methods are unreliable and they also lose performance if used for nonlinear models of the systems.

Different works have evaluated methods of rotor speed estimation. In [9,10], the MRAS method was applied to estimate the rotor speed. Moreover, the rotor speed in an induction machine drive was given as an unknown constant value and an extended Kalman filter was applied in the estimation process [11,12]. The authors of [13] applied the least square method to find out the estimated value of the rotor speed where the best fits interpolated measured signals of an induction machine with dynamic equations.

On the other hand, Walsh functions can be applied in order to study differential equations and dynamic systems efficiently [14,15]. Walsh functions are one of the piecewise constant basis functions [16], which can be applied in problem solving, e.g., optimization control, parameter identification, image processing, communication, and harmonic elimination [17–19]. Walsh functions simplify the solution of nonlinear equations while their piecewise properties decrease noise effects in the ultimate answer. In order to simplify and speed up the solving process, an operational matrix can be used [20].

This paper presents a new online vector control scheme for induction motors that observes the rotor flux orientation directly from machine equations without the need for rotor resistance knowledge. This method applies stator current and voltage as input signals and thereafter estimates motor speed and observes the rotor flux orientation. This process takes place in the Walsh domain with the help of operational matrices, since the motor is analyzed at high speed in time intervals instead of taking samples. Individual characteristics of the applied method diminish noise effects. In the end, as a pseudoinverse method is applied, the response gets more reliable and precise.

2. Vector control in induction machines

In order to apply the system under control based on identifying needed parameters, the first essential step is to have a simple and proper model of each involved component. In this section, an appropriate model for an induction machine in different reference frames is defined.

3. Model of induction machines in arbitrary reference frame

This subsection elaborates the model of an induction machine in an arbitrary reference frame that rotates at angular speed of $\omega_e(\alpha - \beta\,\text{frame})$. In this arbitrary reference frame (Figure 1), the direct and quadratic components of the stator and the rotor voltage equations of an induction machine can be stated as follows [1].

$$\begin{aligned} v_{s\alpha} &= R_s i_{s\alpha} + \dot{\psi}_{s\alpha} - \omega_e \psi_{s\beta} \\ v_{s\beta} &= R_s i_{s\beta} + \dot{\psi}_{s\beta} + \omega_e \psi_{s\alpha} \end{aligned} \tag{1}$$

$$\begin{aligned} 0 &= R_r i_{r\alpha} + \dot{\psi}_{r\alpha} - (\omega_e - \omega_r)\,\psi_{r\beta} \\ 0 &= R_r i_{r\alpha} + \dot{\psi}_{r\beta} + (\omega_e - \omega_r)\,\psi_{r\alpha} \end{aligned} \tag{2}$$

Here, $v_{s\alpha}$ and $v_{s\beta}$ are real and imaginary components of the stator voltage, and $i_{r\alpha}, i_{r\beta}, i_{s\alpha}$, and $i_{s\beta}$ are two components of the rotor and stator currents, respectively. These components are shown in Figure 1. In Eq. (2), R_r and R_s are respectively the resistance for the rotor and stator and $\psi_{r\alpha}$, $\psi_{r\beta}$, $\psi_{s\alpha}$, and $\psi_{s\beta}$ are respectively two components of the rotor and stator fluxes, which can be determined as follows.

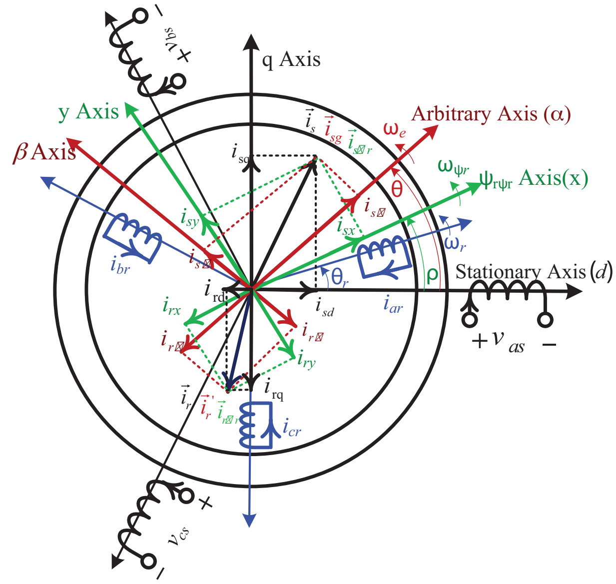

Figure 1. Different reference frames in an induction machine.

$$\begin{aligned} \psi_{s\alpha} &= L_{ls} i_{s\alpha} + L_m(i_{s\alpha} + i_{r\alpha}) \\ \psi_{s\beta} &= L_{ls} i_{s\beta} + L_m(i_{s\beta} + i_{r\beta}) \end{aligned} \tag{3}$$

$$\begin{aligned} \psi_{r\alpha} &= L_{lr} i_{r\alpha} + L_m(i_{s\alpha} + i_{r\alpha}) \\ \psi_{r\beta} &= L_{lr} i_{r\beta} + L_m(i_{s\beta} + i_{r\beta}) \end{aligned} \tag{4}$$

Here, L_{lr}, L_{ls}, and L_m are the leakage inductances of the rotor and stator coils and the mutual inductance between stator and rotor coils per unit, respectively. Eqs. (1) and (2) describe two-phase modeling of the stator and rotor voltage equations in an arbitrary reference frame. Having a squirrel cage rotor causes the components of the rotor voltage to be zero since the rotor voltage equations take the form of Eq. (2). Eqs. (1) through (4) are illustrated in real and imaginary parts, which are very useful for designing the controller and estimation algorithm of the induction machines.

Simultaneous positions of reference frames are shown in Figure 1, where $\vec{i}_s$, $\vec{i}_{sg}$, and $\vec{i}_{s\psi r}$ are the space phasor of the stator current in the stationary, arbitrary, and rotor flux reference frames; ρ is the angle between the stationary and rotor flux reference frames; and $\vec{i}_r$, $\vec{i}_{rg}$, and $\vec{i}_{r\psi r}$ are the space phasors of the rotor current in the stationary, arbitrary, and rotor flux reference frames, respectively.

It can be inferred from Figure 1 that the rotor frame is ahead of the stator frame by an angle of θ_r, mentioning the stator frame as the stationary reference frame, which is defined as the beginner. In these equations, the rotor frame rotates at an angular speed of ω_r, which can be introduced by the electromechanical equation for an induction machine as follows.

$$\dot{\theta}_r = \omega_r \tag{5}$$

$$J\dot{\omega}_r + B\omega_r = P(T_e - T_L) \tag{6}$$

Here, P and T_l are the number of paired poles and load torque, and T_e is the electromagnetic torque in an induction machine, which can be determined as follows.

$$\begin{aligned} T_e &= \tfrac{3P}{2} L_m \left(i_{r\alpha} i_{s\beta} - i_{s\alpha} i_{r\beta} \right) \\ &= \tfrac{3P}{2} \tfrac{L_m}{L_r} \vec{\psi}_{rg} \times \vec{i}_{sg} \end{aligned} \tag{7}$$

Here, $\vec{\psi}_{rg}$ is the vector of the rotor flux in the arbitrary reference frame.

4. Rotor flux-oriented control

The vector form of the variables can be substituted into Eq. (2) to determine a space phasor of the rotor voltage relation of an induction machine as follows.

$$0 = R_r \vec{i}_{r\psi r} + \dot{\vec{\psi}}_{r\psi r} + j \left(\omega_{\psi r} - \omega_r \right) \vec{\psi}_{r\psi r} \tag{8}$$

Here, $\vec{\psi}_{r\psi r}$ is the space phasor of the rotor flux in the rotor-flux reference frame. Combining Eqs. (3) and (4), the space phasor of the rotor flux in the rotor flux reference frame can be obtained by the following.

$$\vec{\psi}_{r\psi r} = L_{lr} \vec{i}_{r\psi r} + L_m (\vec{i}_{s\psi r} + \vec{i}_{r\psi r}) \tag{9}$$

Because the rotor flux reference frame is aligned with rotor flux, $\vec{\psi}_r$ is real and we can write the following.

$$\vec{\psi}_{r\psi r} = \left| \vec{\psi}_{r\psi r} \right| = \psi_{r\psi r} \tag{10}$$

By combining Eqs. (8) and (9) to (10) and resolving the result into real and imaginary components, the modulus and angular speed of the rotor flux space phasor can be obtained as follows.

$$T_r \dot{\psi}_{r\psi r} + \psi_{r\psi r} = L_m i_{sx} \tag{11}$$

$$\omega_{\psi r} = \omega_r + \frac{L_m i_{sy}}{T_r \psi_{r\psi r}} \tag{12}$$

Here, T_r is the time constant of the rotor circuit, which is as follows.

$$T_r = \frac{L_r}{R_r} \tag{13}$$

The simultaneous position of the rotor flux (ρ) can be determined by using the angular speed of the rotor flux $(\omega_{\psi r})$ in Eq. (12) as follows.

$$\dot{\rho} = \omega_{\psi r} \tag{14}$$

Mentioning Eq. (11), the recommended signal for the direct component of the stator current $(\hat{i}_{sx})$ in the steady state can be calculated from the following.

$$\hat{i}_{sx} = \frac{\psi_{rc}}{L_m} \tag{15}$$

Here, ψ_{rc} is the out signal of the flux controller. The quadratic component of the stator current $(\hat{i}_{sy})$ for producing torque reference (T_{ref}) in the rotor flux frame can be obtained from Eq. (7) as follows.

$$\hat{i}_{sy} = \frac{2}{3P}\frac{L_r T_{ref}}{L_m \psi_{r\psi r}} \tag{16}$$

As Figure 2 shows, the rotor flux-oriented control can be performed by applying Eqs. (15) and (16).

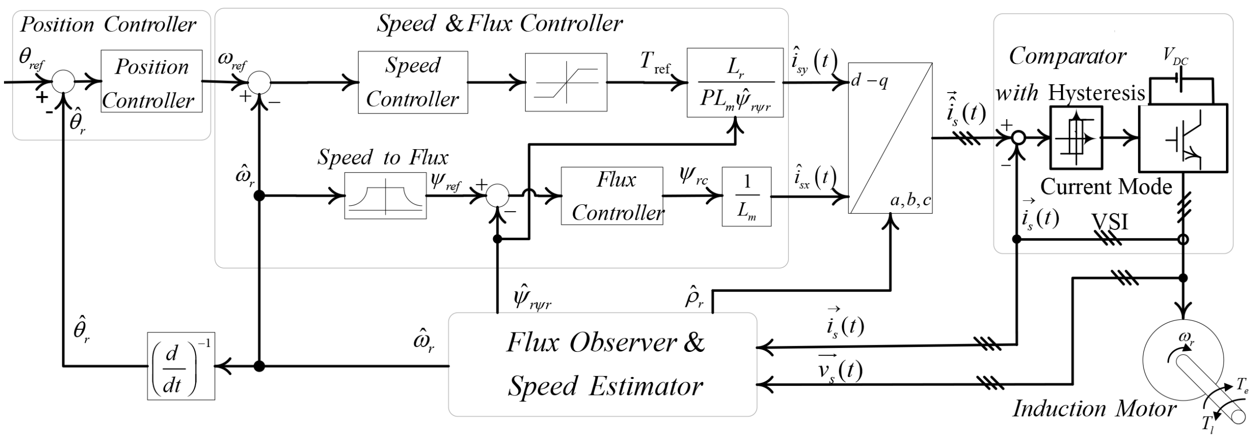

Figure 2. Rotor flux-oriented control of an induction machine.

5. Rotor flux observation and speed estimation

Here the observation and estimation processes will be investigated in the stator reference frame $(d-q)$ where ω_e in Eq. (1) will be substituted with zero. First the manner of calculating components of the rotor flux vector using the stator and rotor components will be studied; applying produced components, this method estimates the unknown rotor speed. Using each two components of Eq. (1) and then integrating them, we will have the following.

$$\psi_{sd} = \int \lim_{0}^{t} (v_{sd} - R_s i_{sd})\, dt + \psi_{sd}(0) \tag{17}$$

$$\psi_{sq} = \int \lim_{0}^{t} (v_{sq} - R_s i_{sq})\, dt + \psi_{sq}(0) \tag{18}$$

Here, $\psi_{sd}(0)$ and $\psi_{sq}(0)$ are two initial values of the stator flux in the stationary reference frame. Real components of the stator and rotor fluxes $(\psi_{sd}$ and $\psi_{sq})$ can be determined by the following.

$$\psi_{sd} = L_{ls} i_{sd} + L_m (i_{sd} + i_{rd}) \tag{19}$$

$$\psi_{rd} = L_{lr} i_{rd} + L_m (i_{sd} + i_{rd}) \tag{20}$$

By eliminating i_{rd} in Eqs. (19) and (20), we have the following.

$$\psi_{sd} = L_s^{'} i_{sd} - \psi_{rd} \tag{21}$$

Here, $L_s^{'}$ is the transient inductance of the induction machine, which can be obtained by the following.

$$L_s' = L_{ls} + \frac{L_{lr} L_m}{L_{lr} + L_m} \tag{22}$$

By substituting Eq. (21) into Eq. (17), we can get the following.

$$\psi_{rd} = \int \lim_0^t (v_{sd} - R_s i_{sd})\, dt + \psi_{sd}(0) - L_s' i_{sd} \tag{23}$$

Similarly, by eliminating i_{rq} from the relations between imaginary components of the stator and rotor fluxes (ψ_{sq} and ψ_{rq}) and substituting results into Eq. (18), we can write the following.

$$\psi_{rq} = \int \lim_0^t (v_{sq} - R_s i_{sq})\, dt + \psi_{sq}(0) - L_s' i_{sq} \tag{24}$$

Based on Eqs. (23) and (24), we can estimate the real and imaginary components of the rotor flux vector in the stationary reference frame ($\hat{\psi}_{rd}$ and $\hat{\psi}_{rq}$). Thus, regarding Figure 1, the quantity and position of the rotor flux in the stationary reference frame can be obtained from the following.

$$\hat{\psi}_{r\psi_r} = \sqrt{\psi_{rd}^2 + \psi_{rq}^2} \tag{25}$$

$$\hat{\rho} = \tan^{-1}\left(\frac{\psi_{rd}}{\psi_{rq}}\right) \tag{26}$$

Eqs. (25) and (26) make the rotor flux vector a known value that can be used in order to compute the rotor speed and position. Moreover, the simultaneous values of the rotor resistance and rotor speed can be estimated by stator currents and voltages in the stationary reference frame. Therefore, by substituting i_{rd} from Eq. (20) into the real component of Eq. (2) in the stationary reference frame, we can conclude the following.

$$R_r \int \lim_0^t \left(\frac{L_m}{L_r} i_{sd} - \frac{1}{L_r}\psi_{rd}\right) dt - \omega_r \int \lim_0^t \psi_{rq} dt = \psi_{rd} - \psi_{rdi} \tag{27}$$

Similarly, by eliminating i_{rq} from the imaginary component in Eq. (2) in the stationary reference frame, we have the following.

$$R_r \int \lim_0^t \left(\frac{L_m}{L_r} i_{sq} - \frac{1}{L_r}\psi_{rq}\right) dt + \omega_r \int \lim_0^t \psi_{rd} dt = \psi_{rq} - \psi_{rqi} \tag{28}$$

The last presented equation can be restated in matrix form as:

$$\begin{bmatrix} H_{11} & H_{12} \\ H_{21} & H_{12} \end{bmatrix} \begin{bmatrix} R_r \\ \omega_r \end{bmatrix} = \begin{bmatrix} U_1 \\ U_2 \end{bmatrix}, \tag{29}$$

in which we have the following.

$$\begin{aligned} &H_{11} = \int \lim_0^t \left(\tfrac{L_m}{L_r} i_{sd} - \tfrac{1}{L_r}\psi_{rd}\right) dt H_{12} = -\int \lim_0^t \psi_{rq} dt \\ &H_{21} = \int \lim_0^t \left(\tfrac{L_m}{L_r} i_{sq} - \tfrac{1}{L_r}\psi_{rq}\right) dt H_{22} = \int \lim_0^t \psi_{rd} dt \\ &U_1 = \psi_{rd} - \psi_{rdi} U_2 = \psi_{rq} - \psi_{rqi} \end{aligned} \tag{30}$$

In order to produce the optimal estimation out of Eq. (29), this paper applies the least square method [21], which minimizes the estimation process error. As can be seen, the least square estimation values for $\hat{R}_r$ and $\hat{\omega}_r$ can be obtained from the following.

$$\begin{bmatrix} \hat{R}_r \\ \hat{\omega}_r \end{bmatrix} = \left(\begin{bmatrix} H_{11} & H_{12} \\ H_{21} & H_{22} \end{bmatrix}^T \begin{bmatrix} H_{11} & H_{12} \\ H_{21} & H_{22} \end{bmatrix} \right)^{-1} \begin{bmatrix} H_{11} & H_{12} \\ H_{21} & H_{22} \end{bmatrix}^T \begin{bmatrix} U_1 \\ U_2 \end{bmatrix} \tag{31}$$

Getting to estimation values from Eq. (31) requires us to solve integral equations; here we apply the Walsh series to find algebraic relations for the estimation of rotor resistance and speed.

6. Estimating rotor resistance and speed by Walsh series

In this section, the properties in the Appendix will be applied in order to solve the dynamic equations used in Eqs. (23), (24), and (31). As a result, the rotor speed and the rotor resistance values will be estimated taking advantage of the Walsh series. First, assuming that the voltage and current of the stator are known signals, transformation of the signals to the Walsh domain takes advantage of Eqs. (A.2), (A.3), and (A.4). According to Eq. (A.3), it is necessary to get an integral of the signal over $t \in [t_s, t_f)$ in order to define its Walsh coefficient in Eq. (A.4), where t_s stands for the start time of each process interval and t_f shows the end of them. Based on the order of the Walsh series, each process interval can be divided into n subintervals. In order to find the arrays of Eq. (A.4) the integral of the signal in each subinterval will be computed. Thereafter, arrays attributed to each Walsh function can be obtained from the sum of all quantities, where the quantity will be negative or positive based on the sign of that function in the mentioned subinterval. Finally, the definition of real and imaginary components of signals with the Walsh series will be as follows.

$$v_{sd} = \mathbf{c}_{vsd}^T \mathbf{w}(t) \quad v_{sq} = \mathbf{c}_{vsq}^T \mathbf{w}(t) \tag{32}$$

$$i_{sd} = \mathbf{c}_{isd}^T \mathbf{w}(t) \quad i_{sq} = \mathbf{c}_{isq}^T \mathbf{w}(t) \tag{33}$$

Using the operational matrix in Eq. (A.8) and combining Eqs. (32) and (33) with Eqs. (23) and (24), the Walsh coefficient vectors' real and imaginary components of the stator flux can be obtained as follows.

$$\mathbf{c}_{\hat{\psi} sd} = E^T \left(\mathbf{c}_{vsd} - R_s \mathbf{c}_{isd} \right) + \mathbf{c}_{\hat{\psi} sd0} \tag{34}$$

$$\mathbf{c}_{\hat{\psi} sq} = E^T \left(\mathbf{c}_{vsq} - R_s \mathbf{c}_{isq} \right) + \mathbf{c}_{\hat{\psi} sq0} \tag{35}$$

Here, $\mathbf{c}_{\hat{\psi} sd}$ and $\mathbf{c}_{\hat{\psi} sq}$ are Walsh coefficient vectors for two components of the stator flux, and $\mathbf{c}_{\hat{\psi} sd0}$ and $\mathbf{c}_{\hat{\psi} sq0}$ are constant initial values of the stator flux components, which are zero for the starting conditions. With Eqs. (23), (24), (34), and (35), the Walsh coefficient vectors for the two components of the rotor flux can be obtained as follows.

$$\mathbf{c}_{\hat{\psi} rd} = E^T \left(\mathbf{c}_{vsd} - R_s \mathbf{c}_{isd} \right) + \mathbf{c}_{\hat{\psi} sd0} - L'_s \mathbf{c}_{isd} \tag{36}$$

$$\mathbf{c}_{\hat{\psi} rq} = E^T \left(\mathbf{c}_{vsq} - R_s \mathbf{c}_{isq} \right) + \mathbf{c}_{\hat{\psi} sq0} - L'_s \mathbf{c}_{isq} \tag{37}$$

These relations can be used for determination of direct and quadrature components of the rotor flux in the stationary reference frame on $t \in [t_s, t_f)$. Thus, at $t = t_f^-$, we have the following.

$$\psi_{rd}(t_f^-) = \mathbf{c}_{\hat{\psi}rd}^T \mathbf{w}(t_f^-) \tag{38}$$

$$\psi_{rq}(t_f^-) = \mathbf{c}_{\hat{\psi}rq}^T \mathbf{w}(t_f^-) \tag{39}$$

Here, t_f^- means approaching t_f from below. By substituting Eqs. (38) and (39) into Eqs. (25) and (26), the amplitude and position of the rotor flux can be obtained as follows.

$$\hat{\psi}_{r\psi_r} = \left(\mathbf{c}_{\hat{\psi}rd}^T \mathbf{w}(t_f^-) \mathbf{w}^T(t_f^-) \mathbf{c}_{\hat{\psi}rd} + \mathbf{c}_{\hat{\psi}rq}^T \mathbf{w}(t_f^-) \mathbf{w}^T(t_f^-) \mathbf{c}_{\hat{\psi}rq} \right)^{\frac{1}{2}} \tag{40}$$

$$\hat{\rho} = \tan^{-1} \left(\frac{\mathbf{c}_{\hat{\psi}rd}^T \mathbf{w}(t_f^-)}{\mathbf{c}_{\hat{\psi}rq}^T \mathbf{w}(t_f^-)} \right) \tag{41}$$

The initial value for the first time interval is zero. The initial value for each interval is the ultimate value for the last interval. Thereafter, having the above variables in the Walsh domain, the optimal estimation in Eq. (31) can be obtained as:

$$\begin{bmatrix} \hat{R}_r \\ \hat{\omega}_r \end{bmatrix} = \left(\hat{\mathbf{H}}^T \hat{\mathbf{H}} \right)^{-1} \hat{\mathbf{H}}^T \hat{u}, \tag{42}$$

in which we have the following.

$$\hat{\mathbf{H}} = \frac{1}{L_r} \begin{bmatrix} \mathbf{E}^T \left(L_m \mathbf{c}_{isd} - \mathbf{c}_{\hat{\psi}rd} \right) & -L_r \mathbf{E}^T \mathbf{c}_{\hat{\psi}rq} \\ L_r \mathbf{E}^T c_{\hat{\psi}rd} & \mathbf{E}^T \left(L_m \mathbf{c}_{isq} - \mathbf{c}_{\hat{\psi}rq} \right) \end{bmatrix} \tag{43}$$

$$\hat{u} = \begin{bmatrix} c_{\hat{\psi}rd} - c_{\hat{\psi}rd0} \\ c_{\hat{\psi}rq} - c_{\hat{\psi}rq0} \end{bmatrix} \tag{44}$$

In this section, the estimation process was elaborated in the Walsh domain. Figure 3 shows the closed-loop speed controlled for an induction machine where the rotor speed estimator is implemented from Eq. (42) by Walsh functions. In order to have better insight about this process, the next section is allocated to a case study on the estimation of the speed and resistance of the rotor.

7. Illustrative example

This section illustrates the estimation process on one time interval ($\Delta t = 5$ ms) and uses a 2-order Walsh series ($k = 2$) in order to evaluate the method. In this section, the machine and controller parameters are as introduced in Table 1.

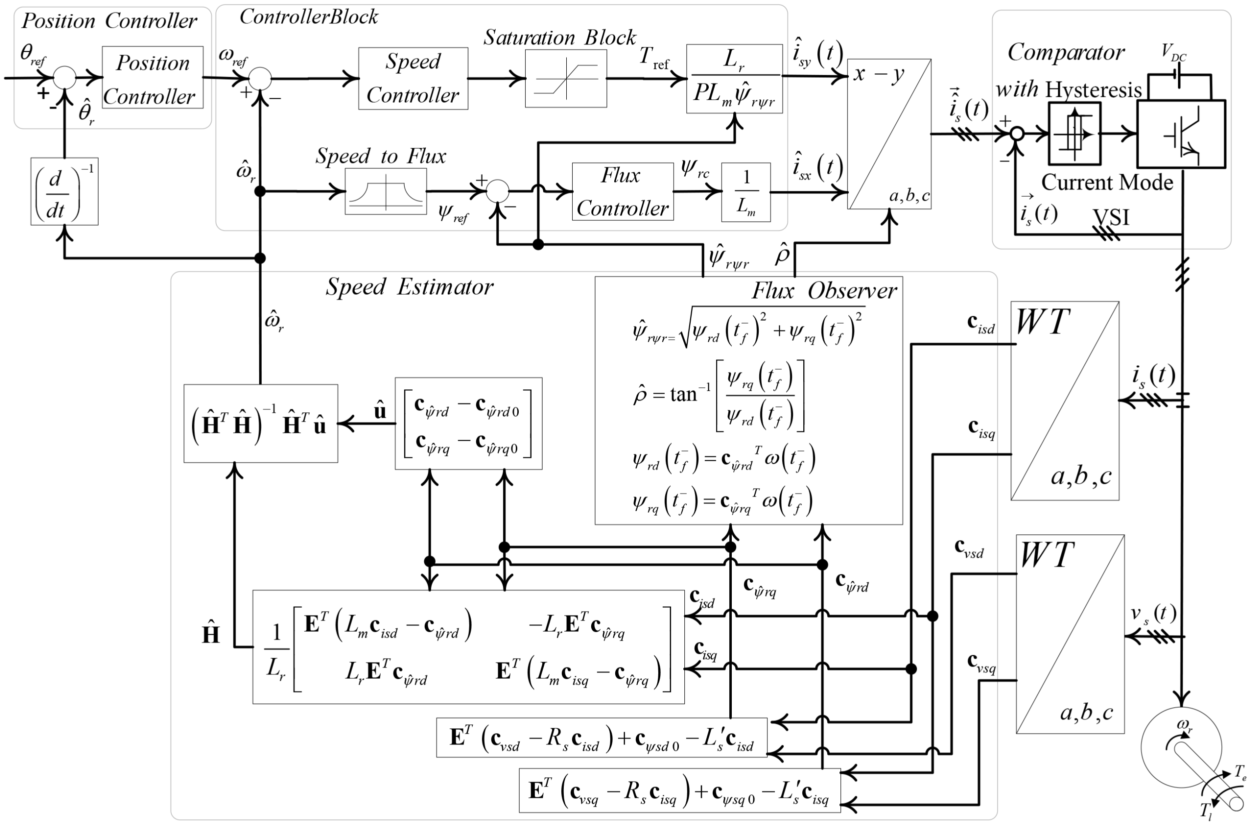

Figure 3. Rotor flux-oriented control of an induction machine in Walsh domain.

Table 1. Induction machine and controller parameters.

Parameter	Symbol	Quantity
Rated power	P_n	1.1. kW
Rated line voltage	P_{II}	415 V
Rated current	I_n	2.77 A
Rated speed	P	1415 RPM
Poles	N_n	4
Stator resistance	R_s	6.03 Ω
Stator leakage inductance	L_{is}	29.3 mH
Rotor leakage inductance	L_{ir}	29.3 mH
Magnetizing inductance	L_{in}	489.3 mH
Moment of inertia	J	0.0517 kgm^2
Friction coefficient	B	0
Speed proportional gain	K_{pw}	0.3
Speed integral gain	K_{iw}	4
Position proportional gain	$K_{p\theta}$	35
Position integral gain	$K_{i\theta}$	500
Flux proportional gain	K_{pf}	1.7
Flux integral gain	K_{if}	3.4

Variation of the rotor resistance is given as follows.

$$R_r = \begin{cases} 6.0850 & t \leq 0.1 \\ 4t + 2.0850 & 0.1 \leq t \leq 0.2 \\ 8.5190 & t \geq 0.2 \end{cases} \tag{45}$$

In this process, voltages and currents of the stator are known as input values. Hence, the Walsh coefficient vectors of real and imaginary components of these signals are available. With this preface, the coefficient vectors for each component of Eqs. (36) and (37) in milliwebers can be written as follows.

$$c_{\hat{\psi}_{rd}} = \begin{bmatrix} 0.1c_0^{v_{sd}} - 61.0c_0^{i_{sd}} + 0.1c_1^{v_{sd}} - 0.3c_1^{i_{sd}} + 1059.9c_0^{\hat{\psi}_{sd0}} \\ -0.1c_0^{v_{sd}} + 0.3c_0^{i_{sd}} - 60.4c_1^{i_{sd}} \end{bmatrix} \tag{46}$$

$$c_{\hat{\psi}_{rq}} = \begin{bmatrix} 0.1c_0^{v_{sq}} - 61.0c_0^{i_{sq}} + 0.1c_1^{v_{sq}} - 0.3c_1^{i_{sq}} + 1059.9c_0^{\hat{\psi}_{sqi}} \\ -0.1c_0^{vsq} + 0.3c_0^{i_{sq}} - 60.4c_1^{i_{sq}} \end{bmatrix} \tag{47}$$

Substituting Eqs. (46) and (47) into Eqs. (43) and (44), we have the following.

$$\begin{bmatrix} 0.9(c_0^{i_{sd}} - c_1^{\hat{\psi}_{rd}}) - 1.9c_0^{\hat{\psi}_{rd}} + 0.4c_1^{i_{sd}} & -c_0^{\hat{\psi}_{rq}} - 0.5c_1^{\hat{\psi}_{rq}} \\ -0.5c_0^{i_{sd}} + c_0^{\hat{\psi}_{rd}} & 0.5c_0^{\hat{\psi}_{rq}} \\ 0.9(c_0^{i_{sq}} - c_1^{\hat{\psi}_{rq}}) - 1.9c_0^{\hat{\psi}_{rq}} + 0.4c_1^{i_{sq}} & c_0^{\hat{\psi}_{rd}} + 0.5c_1^{\hat{\psi}_{rd}} \\ -0.5c_0^{i_{sq}} + c_0^{\hat{\psi}_{rq}} & -0.5c_0^{\hat{\psi}_{rd}} \end{bmatrix} \begin{bmatrix} \hat{R}_r \\ \hat{\omega}_r \end{bmatrix} = 10^4 \begin{bmatrix} c_0^{\hat{\psi}_{rd}} - c_0^{\hat{\psi}_{rd0}} \\ c_1^{\hat{\psi}_{rd}} \\ c_0^{\hat{\psi}_{rq}} - c_0^{\hat{\psi}_{rq0}} \\ c_1^{\hat{\psi}_{rq}} \end{bmatrix} \tag{48}$$

For an evaluation of the estimation method, the matrix relation in Eq. (48) will be extracted in $t = 0.1$ s. In this moment, the Walsh coefficients of the voltages and currents of the stator in the induction machine are as follows.

$$\mathbf{c}_{vsd} = \begin{bmatrix} 0 \\ 300 \end{bmatrix} \quad \mathbf{c}_{vsq} = \begin{bmatrix} 0 \\ 300 \end{bmatrix} \tag{49}$$

$$\mathbf{c}_{isd} = \begin{bmatrix} 1.9786 \\ 0.0095 \end{bmatrix} \quad \mathbf{c}_{isq} = \begin{bmatrix} 1.5466 \\ 0.0135 \end{bmatrix} \tag{50}$$

Initial values for the direct and quadrature fluxes in the stationary reference frame are as follows.

$$c_0^{\hat{\psi}_{rd0}} = 0.86138 \tag{51}$$

$$c_0^{\hat{\psi}_{rq0}} = 0.61284 \tag{52}$$

Thereafter, by applying Eq. (48) to (52), we have the following.

$$\begin{bmatrix} -0.31291 & 0.570932 \\ 0.154233 & -0.285547 \\ -0.364699 & -0.808202 \\ 0.179005 & 0.404087 \end{bmatrix} \begin{bmatrix} \hat{R}_r \\ \hat{\omega}_r \end{bmatrix} = \begin{bmatrix} 1.104950 \\ -0.566727 \\ -6.478690 \\ 3.219450 \end{bmatrix} \quad (53)$$

With Eq. (42), the estimated values for the rotor resistance and speed can be determined as follows.

$$\hat{R}_r = 6.0850\Omega \quad (54)$$

$$\hat{\omega}_r = 5.2706\, rad/\sigma \quad (55)$$

Continuing this process, we can find similar results for $\hat{R}_r$ and $\hat{\omega}_r$ through time. Table 2 shows these estimated values by different orders of Walsh functions.

Table 2. Estimated rotor resistance and speed by Walsh functions with different orders.

Time	Rotor resistance	Estimated rotor		Rotor speed		Estimated rotor	
(s)	$R_r(\Omega)$	Resistance $\hat{R}_r(\Omega)$		ω_r (rad/s)		Speed ω_r (rad/s)	
		$k = 2$	$k = 4$	$k = 2$	$k = 4$	$k = 2$	$k = 4$
0.10	6.0850	6.0850	6.0850	5.0972	5.1115	5.2706	5.2763
0.12	6.5718	6.4478	6.4575	3.4820	3.4715	4.0230	4.0354
0.14	7.0586	6.9450	6.9374	1.2513	1.2482	1.8979	1.9057
0.16	7.5454	7.4252	7.4126	–0.9237	–0.9241	–0.4006	–0.3846
0.18	8.0322	7.9047	7.8949	–2.4916	–2.4914	–2.2088	–2.1882
0.20	8.5190	8.3948	8.3661	–3.1006	–3.1224	–3.2173	–3.2556

8. Simulation results

This section studies the system performance under different conditions. The machine used in these simulations has parameters the same as those in Table 1. The reference value has been set as 0.1 rad for the desirable position and 1 Wb has been taken as rated flux. For examining the efficiency of the system performance under rotor resistance variation this value was set to 1.4 times its preliminary value. This increment started to take part in 0.1 s with a ramp pattern of which the controller was completely unaware. In this study, the 4-order Walsh series was applied and new estimated values were uploaded to controller in each 5 ms. By operating the motor as seen in Figure 3, the controller started to estimate the rotor flux and took advantage of that in order to estimate the rotor speed, which was used in estimation of the rotor position. These estimated values helped the closed-loop controller in making the motor follow its references. Figure 4 shows the performance of the system under unit and ramp changes of the reference value.

In Figure 4a, it can be seen that the motor has started to run with making its flux, which gets to the rated value and sticks to it. It can be seen that under alteration of the reference value the quantity of the flux will not change and the position of the rotor flux vector will be in charge of adaptation. Figure 4b illustrates the mechanical output of the system under the mentioned variation of the reference. It shows that the motor varies its speed in order to adjust itself with the new desirable position. Here, motor speed fluctuates and settles down when the rotor has reached its position. These results verify the high performance of the proposed estimator in control of induction machines.

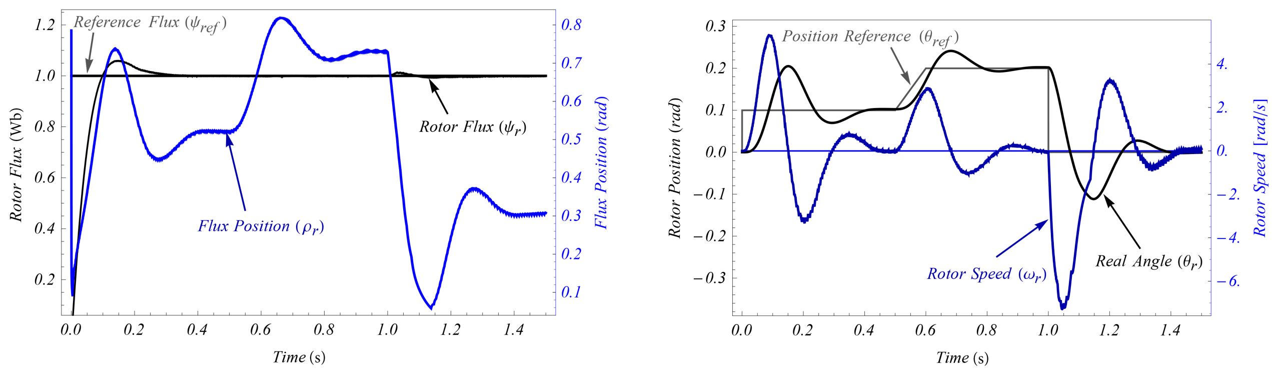

Figure 4. Closed-loop response of the sensorless vector control system with Walsh function estimator.

For a better understanding of estimation process, Figure 5 elaborates the process for speed and position of the rotor flux and the rotor itself. The represented part occurs during the increment of the rotor resistance value.

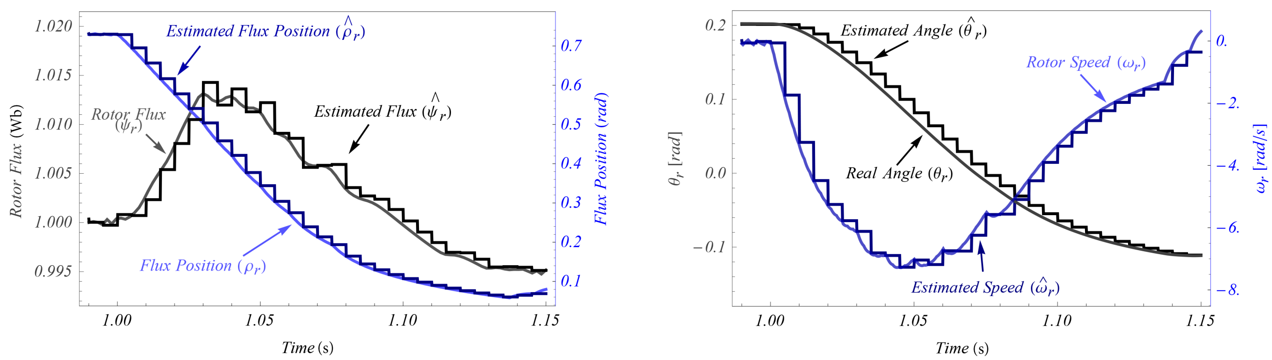

Figure 5. Real and estimated values.

Here, Walsh functions have been defined in time intervals of 100 μ s and the estimation process was done in this period. Achieving the estimated values, these quantities were saved and used for the next 4.9 ms. This means that needed values could be updated after each 5 ms. A higher order of Walsh series and smaller period of processing time can be chosen based on the need for a more precise answer.

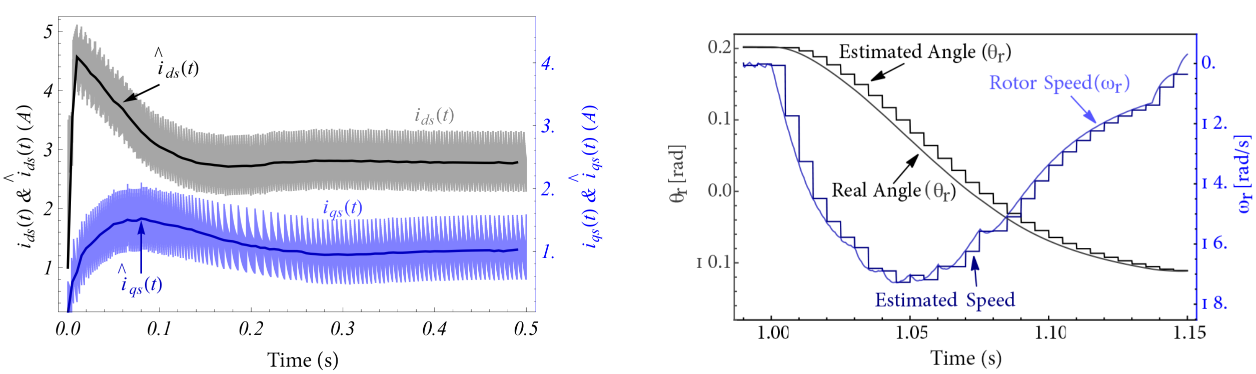

Figure 6. Two components of the stator voltages and currents.

6 shows the stator voltages and currents under switching mode. These patterns happen due to nonlinear characteristics of induction machines. As can be seen, these signals with high harmonics are not considered a big deal for the estimation process.

9. Conclusions

The development of a high-performance sensorless RFOC of an induction machine that is insensitive to rotor resistance variation has been addressed in this paper. This method needed the induction machine to be modeled in the Walsh domain; hence, the evaluation process became simpler and sped up in respect to application of the operational matrix. Applying the stator voltage and current as input values, the rotor flux space vector was observed and used in order to estimate motor speed. Finally, the system applied the provided values to produce the needed signals to feed the motor in order to adjust the position of the induction motor in the rotor flux-oriented control. The validity of the proposed method was illustrated in some simulation results, which showed the excellent performance of the system and its capability of reducing noise effects.

References

[1] Vas P. Sensorless Vector and Direct Torque Control. New York, NY, USA: Oxford University Press, 1998.

[2] Lee GS, Lee DH, Yoon TW, Lee KB, Song JH, Choy I. Speed and flux estimation for an induction motor using a parameter estimation technique. Int J Control Autom 2005; 3: 79-86.

[3] Miloudi A, Al-Radadi EA, Draou AD. A variable gain PI controller used for speed control of a direct torque neuro fuzzy controlled induction machine drive. Turk J Electr Eng Co 2007; 15: 37-49.

[4] Karanayil B, Rahman MF, Grantham C. Stator and rotor resistance observers for induction motor drives using fuzzy logic and artificial neural networks. IEEE T Energy Conver 2005; 20: 771-780.

[5] Lorenz RD, Lawson DB. A simplified approach to continuous on-line tuning of field oriented induction motor drives, IEEE T Ind Appl 1991; 26: 420-424.

[6] Krishnan R, Bharadwaj AS. A review of parameter sensitivity and adaption in indirect vector controlled induction motor drives. IEEE T Power Electr 1991; 6: 695-703.

[7] Lai LC, Demarco CL, Lipo TA. An extended Kalman filter approach to rotor time constant measurement in PWM induction motor drives. IEEE T Ind Appl 1992; 28: 96-104.

[8] Ozsoy EE, Gokasan M, Bogosyan S. Simultaneous rotor and stator resistance estimation of squirrel cage induction machine with a single extended Kalman filter. Turk J Electr Eng Co 2010; 18: 853-863.

[9] Tajima H, Hori Y. Speed sensorless field-orientation control of the induction machine. IEEE T Ind Appl 1993; 29: 175-180.

[10] Peng FZ, Fukao T. Robust speed identification for speed sensorless vector control of induction motors. IEEE T Ind Appl 1994; 30: 1234-1240.

[11] Kim YR, Sui SK, Park HM. Speed sensorless vector control of induction motor using extended Kalman filter. IEEE T Ind Appl 1994; 30: 1225-1233.

[12] Du T, Vas P, Stronach F. Design and application of extended observers for joint state and parameter estimation in high performance AC drives. IEE P-Elect Pow Appl 1995; 142: 71-78.

[13] Reyes MV, Verghese GC. Subset selection in identification, and application to speed and parameter estimation for induction machines. In: Fourth IEEE Conference on Control Application; 28–29 September 1995; Albany, NY, USA. New York, NY, USA: IEEE. pp. 991-971.

[14] Rao GP. Piecewise Constant Orthogonal Functions and Their Application to Systems and Control. Berlin, Germany: Springer-Verlag, 1983.

[15] Chen CF, Hsiao CH. Design of piecewise constant gains for optimal control via Walsh functions. IEEE T Automat Contr 1975; 20: 596-603.

[16] Ajily E, Nazarzadeh J. Piecewise constant orthogonal based estimator in vector controlled drives of induction motors. International Review on Modeling and Simulation 2010; 3: 809-816.

[17] Melgoza JR, Heydt GT, Keyhani A, Agrawal BL, Selin D. An algebraic approach for identifying operating point dependent parameters of synchronous machines using orthogonal series expansions. IEEE T Energy Conver 1991; 16: 420-424.

[18] Lazaridis G, Petrou M. Image registration using the Walsh transform. IEEE T Image Process 2006; 15: 2343-2357.

[19] Windeatt T, Zor C. Minimising added classification error using Walsh coefficients. IEEE T Neural Networ 2011; 22: 334-1339.

[20] Radmanesh HR, Shakouri H, Nazarzadeh J. Synchronous generator parameter estimation using pseudo-inverse method in hybrid domain. In: IEEE 2007 International Symposium on Industrial Electronics; 4–7 June 2007; Vigo, Spain. New York, NY, USA: IEEE. pp. 335-340.

[21] Simon D. Optimal State Estimation, Kalman, H∞, and Non-Linear Approaches. Hoboken, NJ, USA: Wiley, 2006.

[22] Razzaghi M, Nazarzadeh J. Walsh functions. Wiley Encyclopedia of Electrical and Electronic Engineering 1999; 23: 429-440.

Appendix. Walsh series.

Here Walsh functions will be introduced, which help us get an easier solution of dynamical equations. Walsh functions are defined in the time interval of $[0, 1)$ and take the form of an orthogonal set of rectangular functions, and this characteristic diminishes the noise effect. There are different well-known types of ordering for Walsh functions [22]. Figure A.1 shows the set of the first four Walsh functions arranged in Paley order.

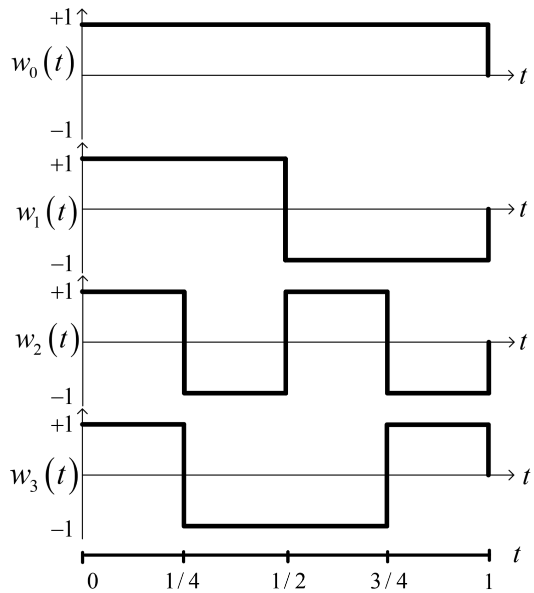

Figure A.1. The first four Walsh functions.

The Walsh functions are orthogonal, and this characteristic explains the following.

$$\int_0^1 w_m(t)\, w_n(t)\, dt = \delta_{mn} \tag{A.1}$$

Here δ_{mn} is the Kronecker delta function. The Walsh functions can even be used on the time interval of $t \in [0, t)$. Mentioning $x(t)$ as a square-integrable signal with smooth variation, it can be restated in the Walsh domain by a finite Walsh series as follows.

$$x(t) \approx \sum \lim_{n=0}^{k-1} c_n^x w_n(t) = \mathbf{c}_x^T \mathbf{w}(t) \tag{A.2}$$

Here, c_n^x is the Walsh coefficient of $x(t)$, which can be obtained by orthogonality property as follows.

$$c_n^x = \int_0^t x(t)\, w_n(t)\, dt, \qquad n = 0, 1, 2, \ldots, k-1 \tag{A.3}$$

$\mathbf{c}_x$ and $\mathbf{w}(t)$ in Eq. (A.2) are two column vectors, which are given as follows.

$$\mathbf{c}_x = \begin{pmatrix} c_0^x & c_1^x & c_2^x & \cdots & c_{k-1}^x \end{pmatrix}^T \tag{A.4}$$

$$\mathbf{w}(t) = \begin{pmatrix} w_0(t) & w_1(t) & w_2(t) & \cdots & w_{k-1}(t) \end{pmatrix}^T \tag{A.5}$$

For square-integrable $x(t)$ and $y(t)$ on the time interval of $t \in [0,t)$, $\mathbf{c}_x$ and $\mathbf{c}_y$ are their Walsh coefficient vectors, respectively, and then we have the following.

$$x\left(t\right) \pm y\left(t\right) \approx \left(\mathbf{c}_x \pm \mathbf{c}_y\right)^T \mathbf{w}(t) \tag{A.6}$$

The effect of the integration function on the Walsh series on the time interval of $t \in [0,t)$ can be written as follows.

$$\int_0^t \mathbf{w}(\tau)d\tau \approx \mathbf{E}\mathbf{w}(t) \tag{A.7}$$

Here, the operational matrix of $\mathbf{E}$ is a $k \times k$ well-defined numerical matrix that can be defined as follows [22].

$$\mathbf{E} = \frac{t}{k}\begin{bmatrix} \frac{1}{2} & \frac{1}{4} & \frac{1}{8} & 0 & & \\ -\frac{1}{4} & 0 & 0 & \frac{1}{8} & \cdots & \\ -\frac{1}{8} & 0 & 0 & 0 & & \frac{1}{2k}\mathbf{I}_{\frac{k}{2}} \\ 0 & -\frac{1}{8} & 0 & 0 & & \\ \vdots & & & & \ddots & \\ \frac{1}{2k}\mathbf{I}_{\frac{k}{2}} & & & & & \mathbf{0}_{\frac{k}{2}} \end{bmatrix} \tag{A.8}$$

Here, $\mathbf{I}_{\frac{k}{2}}$ and $0_{\frac{k}{2}}$ are two $k/2 \times k/2$ squared-identity and zero matrices. Combining Eqs. (A.2) and (A.7), the integral of $x(t)$ can be converted into an algebraic relation as follows.

$$\int_0^t x\left(\tau\right)d\tau = \mathbf{c}_x^T\left(\int_0^t \mathbf{w}(\tau)d\tau\right) \approx \mathbf{c}_x^T\mathbf{E}\mathbf{w}\left(t\right) \tag{A.9}$$